

Cooperative Binding of Phosphate Anion and a Neutral Nitrogen Donor to Alkaline-Earth Metal Ions. Investigation of Group 2 Metal–Organophosphate Interaction in the Absence and Presence of 1,10-Phenanthroline

Ramaswamy Murugavel,* Subramaniam Kuppaswamy, and Sören Randoll

Department of Chemistry, Indian Institute of Technology—Bombay, Powai, Mumbai 400076, India

Received February 20, 2008

Alkaline-earth metal phosphates containing nitrogen-donor ligands have been prepared by the reaction of alkaline-earth metal acetates $M(\text{OAc})_2 \cdot x\text{H}_2\text{O}$ ($M = \text{Mg}, \text{Ca}, \text{Sr}, \text{Ba}$) with 2,6-diisopropylphenyl phosphate (dippH_2) in the absence and presence of 1,10-phenanthroline (phen). Interaction of strontium or barium acetate with dippH_2 in methanol at room temperature leads to the isolation of ionic phosphates $[\{M_2(\mu\text{-H}_2\text{O})_4(\text{H}_2\text{O})_{10}\}\{\text{dipp}\}_2] \cdot 4\text{L}$ [$M = \text{Sr}, \text{L} = \text{CH}_3\text{OH}$ (**1**); $M = \text{Ba}, \text{L} = \text{H}_2\text{O}$ (**2**)]. The addition of a bidentate nitrogen-donor phen to these reactions leads to the isolation of dinuclear metal phosphates $[\text{Mg}(\text{dipp})(\text{phen})(\text{CH}_3\text{OH})_2]_2$ (**3**) and $[\text{M}(\text{dippH})_2(\text{phen})_2(\text{H}_2\text{O})_2]_2$ [$M = \text{Ca}$ (**4**), Sr (**5**), Ba (**6**)]. While ionic phosphates **1** and **2** are soluble in water, the predominately covalent dimeric compounds **3–6** are insoluble in all common solvents including water. The new compounds have been characterized in the solid state by elemental analysis, IR, UV–vis, and emission spectroscopy, and single-crystal X-ray diffraction studies. The cationic part in **1** and **2** is a $\{M_2(\mu\text{-H}_2\text{O})_4(\text{H}_2\text{O})_{10}\}$ unit, where each metal ion is surrounded by four bridging and five terminal water molecules as ligands. The dipp anion does not directly bind to the metal ions but is extensively hydrogen-bonded to the cationic unit through the phosphate oxygen and water hydrogen atoms to result in an infinitely layered structure where the hydrophobic aryl group protrudes out of the hydrophilic layer formed by the cationic part and $-\text{PO}_3^{2-}$ units. In contrast, compounds **3–6** are discrete dimeric molecules built around a central $M_2\text{O}_4\text{P}_2$ eight-membered ring. While the dippH_2 ligand exists in a doubly deprotonated form in **3**, two monodeprotonated dippH_2 ligands are present per metal ion in compounds **4–6**. While **3** prefers only one phen ligand in the metal coordination sphere, two phen ligands chelate each metal ion in **4–6**. The conformations of the eight-membered rings in **3–6** vary significantly from each other depending on the size of the cation and the coordination number around the metal. Further, intermolecular hydrogen bonding involving the phenanthroline C–H linkages result, in a gridlike structure in **1**, one-dimensional chains in isostructural **2** and **3**, and a two-dimensional layer arrangement in **4**. Compounds **3–6** are the only examples of alkaline-earth metal phosphate complexes with neutral M–N donor bonds. The thermal behavior of compounds **1–6** has been examined with the help of thermogravimetric analysis and differential scanning calorimetry and also by bulk thermolysis followed by powder X-ray diffraction measurements. While compounds **1** and **2** yield $M_2\text{P}_2\text{O}_7$, decomposition of **4–6** results in the formation of $M(\text{PO}_3)_2$, consistent with the M–P ratio in the precursor complexes.

Introduction

The design and synthesis of new alkaline-earth metal complexes have received considerable attention because of their potential applications in fields such as catalysis, material

science, and biochemistry.¹ Furthermore, group 2 metal chemistry is determined by the size and charge density of the metal ion² and, thus, varies considerably upon moving down the group. For example, with regard to coordination chemistry, calcium is observed to exhibit coordination numbers ranging from 3 to 9, while the most commonly observed are 6–8, whereas strontium and barium prefer

* To whom correspondence should be addressed. E-mail: rmv@chem.iitb.ac.in. Fax: +91-22-2572 3480.

coordination numbers 6–12.^{1–10} The coordination behavior of alkaline-earth metal cations, especially that of calcium, is a topic of current interest owing to the vital roles that these metal ions play in biological systems.¹¹ Among the alkaline-earth metal complexes, only a small number of phosphates are known in the literature, and this is a surprising fact because the skeleton and teeth of the human body consist of calcium-deficient hydroxyapatite, a calcium phosphate.¹² Structurally characterized magnesium and calcium phosphate complexes are very rare, but at least a noticeable number have been established.^{13,14} However, only one example in each case of strontium and barium dibutylphosphate has been reported so far.^{15,16}

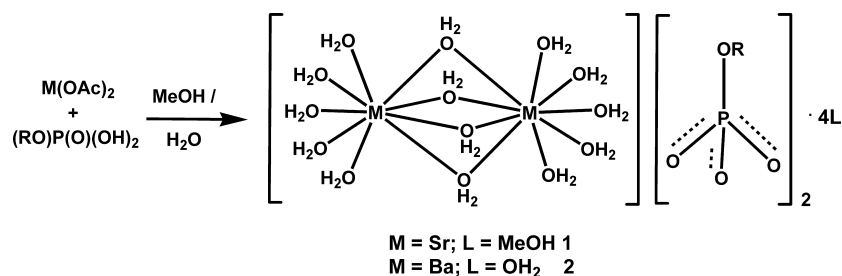
Continuing our interest in the rational assembly of large metallophosphate molecules that could mimic zeolite building blocks^{17–19} and our sustained efforts to unravel the coordination behavior of group 2 metal cations,^{3,4} we present in this contribution the synthesis and structural characterization of

new organophosphates of alkaline-earth metal ions and an account of their solid-state association and thermal behavior. The synthesis of these complexes was carried out in the absence and presence of 1,10-phenanthroline (phen) because it is well-known that chelating ligands inhibit the expansion of polymeric frameworks to give coordination polymers of low-dimensionality or zero-dimensional molecules.^{20,21}

Results and Discussion

The interaction of alkyl- or arylphosphonic acids, RPO₃H₂, with alkaline-earth metal ions has been well investigated in

- (1) (a) Cowan, K. D. U.S. Patent 4,544,767, 1985. (b) Chandler, C. D.; Roger, C.; Hampden-Smith, M. J. *Chem. Rev.* **1993**, *93*, 1205. (c) Boyle, T. J.; Bucheit, C. D.; Rodriguez, M. A.; Al-Shareef, H. N.; Hernandez, B. A.; Scott, B.; Ziller, J. W. *J. Mater. Res.* **1996**, *9*, 2246. (d) Westerhausen, M.; Schneiderbauer, S.; Kneifel, A. N.; Sörtl, Y.; Mayer, P.; Nöth, H.; Zhong, Z.; Dijkstra, P. J.; Feijen, J. *Eur. J. Inorg. Chem.* **2003**, 3432. (e) Fromm, K. M.; Gueneau, E. D. *Polyhedron* **2004**, *23*, 1479. (f) Evans, C. A.; Guerremont, R.; Rabenstein, D. L. *Metal Ions in Biological Systems*; Sigel, H., Ed.; Marcel Dekker: New York, 1979; Vol. 9, p 41. (g) Kendrick, M. J.; May, M. T.; Plishka, M. J.; Robinson, K. D. *Metals in Biological Systems*; Ellis Horwood: New York, 1992; pp 57–65. (h) Doyno, T. *Adv. Protein Chem.* **1966**, *22*, 600. (i) Freeman, H. C. *Inorganic Biochemistry*; Eichhorn, J., Ed.; Marcel Dekker: New York, 1979; Vol. 1, p 129.
- (2) Poonia, N. S.; Bajaj, A. V. *Chem. Rev.* **1979**, *79*, 389.
- (3) (a) Murugavel, R.; Karambelkar, V. V.; Anantharaman, G.; Walawalkar, M. G. *Inorg. Chem.* **2000**, *39*, 1381. (b) Murugavel, R.; Baheti, K.; Anantharaman, G. *Inorg. Chem.* **2001**, *40*, 6870. (c) Murugavel, R.; Kumar, P.; Walawalkar, M. G.; Mathialagan, R. *Inorg. Chem.* **2007**, *46*, 6828. (d) Murugavel, R.; Korah, R. *Inorg. Chem.* **2007**, *46*, 11048.
- (4) (a) Murugavel, R.; Korah, R. *Synth. React. Inorg. Met.–Org. Chem.* **2007**, *37*, 779. (b) Murugavel, R.; Banerjee, S. *Inorg. Chem. Commun.* **2003**, *6*, 810. (c) Murugavel, R.; Karambelkar, V. V.; Anantharaman, G. *Ind. J. Chem., Sect. A* **2000**, *39A*, 843. (d) Murugavel, R.; Anantharaman, G.; Krishnamurthy, D.; Sathiyendiran, M.; Walawalkar, M. G. *Proc.–Ind. Acad. Sci., Chem. Sci.* **2000**, *112*, 273. (e) Krishnamurthy, D.; Murugavel, R. *Ind. J. Chem., Sect. A* **2003**, *42A*, 2267.
- (5) (a) He, X.; Allan, J. F.; Noll, B. C.; Kennedy, A. R.; Henderson, K. W. *J. Am. Chem. Soc.* **2005**, *127*, 6920. (b) Davies, R. P. *Inorg. Chem. Commun.* **2000**, *3*, 13. (c) Feil, F.; Harder, S. *Eur. J. Inorg. Chem.* **2005**, 4438. (d) Avent, A. G.; Crimmin, M. R.; Hill, M. S.; Hitchcock, P. B. *Dalton Trans.* **2005**, 278. (e) Tang, Y.; Zakharov, L. N.; Kassel, W. S.; Rheingold, A. L.; Kemp, R. A. *Inorg. Chim. Acta* **2005**, *358*, 2014. (f) Chisholm, M. H.; Gallucci, J. C.; Phomphrai, K. *Inorg. Chem.* **2004**, *43*, 6717.
- (6) (a) Ullström, A.-S.; Warminska, D.; Persson, I. J. *Coord. Chem.* **2005**, *58*, 611. (b) Crane, J. D.; Moreton, D. J.; Rogerson, E. *Eur. J. Inorg. Chem.* **2004**, *21*, 4237. (c) Sahbari, J. J.; Olmstead, M. M. *Acta Crystallogr., Sect. C* **1983**, *39*, 208. (d) Sohrin, Y.; Kokusen, H.; Kihara, S.; Matsui, M.; Kushi, Y.; Shiro, M. *J. Am. Chem. Soc.* **1993**, *115*, 4128. (e) Sohrin, Y.; Matsui, M.; Hata, Y.; Hasegawa, H.; Kokusen, H. *Inorg. Chem.* **1994**, *33*, 4376. (f) Tesh, K. F.; Burkey, D. J.; Hanusa, T. P. *J. Am. Chem. Soc.* **1994**, *116*, 2409.
- (7) (a) Wörl, S.; Fritsky, I. O.; Hellwinkel, D.; Pritzkow, H.; Krämer, R. *Eur. J. Inorg. Chem.* **2005**, *22*, 759. (b) Reger, D. L.; Little, C. A.; Smith, M. D. *Inorg. Chem.* **2002**, *41*, 19. (c) Hundal, G.; Hundal, M. S.; Obrat, S.; Poonia, N. S.; Kumar, S. *Inorg. Chem.* **2002**, *41*, 2077. (d) Debuyst, R.; Dejehet, F.; Dekandelaer, M. C.; Declerco, J. P.; Germain, G.; Van Meerssche, M. J. *Chim. Phys.* **1979**, *78*, 1117.
- (8) (a) Onoda, A.; Yamada, Y.; Nakayama, Y.; Takahashi, K.; Adachi, H.; Okamura, T.-A.; Nakamura, A.; Yamamoto, H.; Ueyama, N.; Vyprachticky, D.; Okamoto, Y. *Inorg. Chem.* **2004**, *43*, 4447. (b) Chen, X. M.; Mak, T. C. W. *Polyhedron* **1994**, *13*, 1087. (c) Cole, L. B.; Holt, E. M. *Inorg. Chim. Acta* **1989**, *160*, 195.
- (9) (a) Starosta, W.; Leciejewicz, J. *J. Coord. Chem.* **2005**, *58*, 891. (b) Kumar, K.; Tweedle, M. F.; Malley, M. F.; Gougoutas, J. Z. *Inorg. Chem.* **1995**, *34*, 6472. (c) Evans, W. J.; Giarikos, D. G.; Greci, M. A.; Ziller, J. W. *Eur. J. Inorg. Chem.* **2002**, 453. (d) Clegg, W.; Hunt, P. A.; Straughan, B. P.; Mendiola, M. A. *J. Chem. Soc., Dalton Trans.* **1989**, 1127. (e) Waters, A. F.; White, A. H. *Aust. J. Chem.* **1996**, *49*, 27. (f) Waters, A. F.; White, A. H. *Aust. J. Chem.* **1996**, *49*, 87. (g) Kepert, D. I.; Waters, A. F.; White, A. H. *Aust. J. Chem.* **1996**, *49*, 117.
- (10) (a) Côté, A. P.; Shimizu, G. K. H. *Chem.–Eur. J.* **2003**, *9*, 5361. (b) Mezei, G.; Raptis, R. G. *New J. Chem.* **2003**, *27*, 1399. (c) Onoda, A.; Yamada, Y.; Doi, M.; Okamura, T.; Ueyama, N. *Inorg. Chem.* **2001**, *40*, 516.
- (11) (a) Katz, A. K.; Glusker, J. P.; Beebe, S. A.; Bock, C. W. *J. Am. Chem. Soc.* **1996**, *118*, 5752. (b) Hitzbleck, J.; Deacon, G. B.; Ruhlandt-Senge, K. *Angew. Chem., Int. Ed.* **2004**, *43*, 5218.
- (12) Goldwhite, H. *Introduction to Phosphorus Chemistry*; Cambridge University Press: Cambridge, U.K., 1981.
- (13) (a) Ezra, F. S.; Collin, R. L. *Acta Crystallogr., Sect. B* **1973**, *29*, 1398. (b) Ramirez, F.; Sarma, R.; Chaw, Y. F.; McCaffrey, T. M.; Marecek, J. F.; McKeever, B.; Nierman, D. J. *Am. Chem. Soc.* **1977**, *99*, 5285. (c) Narayanan, P.; Ramirez, F.; McCaffrey, T.; Chaw, Y. F.; Marecek, J. F. *J. Org. Chem.* **1978**, *43*, 24. (d) Adams, H.; Rolfe, A.; Jones, S. *Acta Crystallogr., Sect. E* **2005**, *E61*, m1251. (e) Steitz, T. A.; Steitz, J. A. *Proc. Natl. Acad. Sci. U.S.A.* **1993**, *90*, 6498. (f) York, J. D.; Ponder, J. W.; Chen, Z.-W.; Mathews, F. S.; Majerus, P. W. *Biochemistry* **1994**, *33*, 13164. (g) Pelletier, H.; Sawaya, M. R.; Kumar, A.; Wilson, S. H.; Kraut, J. *Science* **1994**, *264*, 1891. (h) Yun, J. W.; Tanase, T.; Lippard, S. J. *Inorg. Chem.* **1996**, *35*, 7590. (i) Bissinger, P.; Kumberger, O.; Schier, A. *Chem. Ber.* **1991**, *124*, 509. (j) Izumi, M.; Ichikawa, K.; Suzuki, M.; Tanaka, I.; Rudzinski Krzysztof, W. *Inorg. Chem.* **1995**, *34*, 5388.
- (14) (a) Onoda, A.; Yamada, Y.; Okamura, T.; Yamamoto, H.; Ueyama, N. *Inorg. Chem.* **2002**, *41*, 6038. (b) Demadis, K. D.; Sallis, J. D.; Raptis, R. G.; Baran, P. J. *Am. Chem. Soc.* **2001**, *123*, 10129.
- (15) Burns, J. H.; Kessler, R. M. *Inorg. Chem.* **1987**, *26*, 1370.
- (16) (a) Kyogoku, Y.; Iitaka, Y. *Acta Crystallogr.* **1966**, *21*, 49. (b) Burns, J. H. *Inorg. Chim. Acta* **1985**, *102*, 15.
- (17) (a) Pothiraja, R.; Sathiyendiran, M.; Butcher, R. J.; Murugavel, R. *Inorg. Chem.* **2005**, *44*, 6314. (b) Pothiraja, R.; Sathiyendiran, M.; Butcher, R. J.; Murugavel, R. *Inorg. Chem.* **2004**, *43*, 7585. (c) Murugavel, R.; Sathiyendiran, M.; Pothiraja, R.; Walawalkar, M. G.; Mallah, T.; Riviere, E. *Inorg. Chem.* **2004**, *43*, 945. (d) Murugavel, R.; Sathiyendiran, M.; Pothiraja, R.; Butcher, R. J. *Chem. Commun.* **2003**, 2546. (e) Sathiyendiran, M.; Murugavel, R. *Inorg. Chem.* **2002**, *41*, 6404. (f) Murugavel, R.; Sathiyendiran, M. *Chem. Lett.* **2001**, 84. (g) Murugavel, R.; Sathiyendiran, M.; Walawalkar, M. G. *Inorg. Chem.* **2001**, *40*, 427. (h) Pothiraja, R.; Shanmugan, S.; Walawalkar, M. G.; Butcher, R. J.; Nethaji, M.; Murugavel, R. *Eur. J. Inorg. Chem.* **2008**, 1834.
- (18) (a) Murugavel, R.; Kuppuswamy, S. *Angew. Chem., Int. Ed.* **2006**, *45*, 7022. (b) Murugavel, R.; Kuppuswamy, S.; Boomishankar, R.; Steiner, A. *Angew. Chem., Int. Ed.* **2006**, *45*, 5536. (c) Murugavel, R.; Kuppuswamy, S. *Chem.–Eur. J.* **2008**, *14*, 3869. (d) Murugavel, R.; Shanmugan, S.; Kuppuswamy, S. *Eur. J. Inorg. Chem.* **2008**, 1508. (e) Murugavel, R.; Walawalkar, M. G.; Pothiraja, R.; Rao, C. N. R.; Choudhury, A. *Chem. Rev.* **2008**, in press.
- (19) (a) Murugavel, R.; Pothiraja, R.; Gogoi, N.; Clerac, R.; Lecren, L.; Butcher, R. J.; Nethaji, M. *Dalton Trans.* **2007**, 2405. (b) Murugavel, R.; Shanmugan, S. *Chem. Commun.* **2007**, 1257. (c) Murugavel, R.; Singh, M. P. *Inorg. Chem.* **2006**, *45*, 9154. (d) Murugavel, R.; Davis, P.; Walawalkar, M. G. *Z. Anorg. Allg. Chem.* **2005**, *631*, 2806. (e) Davis, P.; Murugavel, R. *Synth. React. Inorg. Met.–Org. Chem.* **2005**, *35*, 591.

Scheme 1. Synthesis of **1** and **2** (R = 2,6-*i*-Pr₂C₆H₃)

the last few decades.²² Depending on the type of phosphonic acids and the reaction conditions used (such as pH), two homologous series of group 2 metal phosphonates, $[M(\text{RPO}_3)]$ and $[M(\text{RPO}_3\text{H})_2]$, have been isolated and their structures determined using single-crystal X-ray diffraction studies in representative cases.²² It is now well established that both series of group 2 metal phosphonates form layered solids whose structure resembles very much that of other transition-metal-layered phosphonates.

Phosphonic acids (RPO_3H_2) and phosphate monoesters $[(\text{RO})\text{PO}_3\text{H}_2]$, although structurally similar, behave differently when reacted with the same metal precursor complex. For example, while the reaction of phenylphosphonic acid with zinc acetate affords layered zinc phosphonate $[\text{ZnO}_3\text{PPh}(\text{H}_2\text{O})]_n$,²³ a similar reaction involving 2,6-diisopropylphenyl phosphate (dippH_2) yields several tetrameric clusters $[\text{Zn}(\text{dipp})(\text{L})]_4$ (L = a variety of donor ligands), which have, in fact, been used as building blocks to assemble zeolite-like porous solids.^{18b} Owing to this large difference in the case of zinc, the reactivity pattern of dippH_2 with group 2 metal ions has been investigated in the present study.

Synthesis and Spectra of $[\{M_2(\mu\text{-H}_2\text{O})_4(\text{H}_2\text{O})_{10}\}\{\text{dipp}\}_2] \cdot 4\text{L}$ [M = Sr, L = CH₃OH (1**); M = Ba, L = H₂O (**2**)]**. Equimolar reaction between strontium/barium acetate and dippH_2 in a CH₃OH–H₂O mixture at ambient temperature followed by crystallization yields ionic phosphates $[\{M_2(\mu\text{-H}_2\text{O})_4(\text{H}_2\text{O})_{10}\}\{\text{dipp}\}_2] \cdot 4\text{L}$ [M = Sr, L = CH₃OH (**1**); M = Ba, L = H₂O (**2**)], respectively, in good yields (Scheme

1).²⁴ The products have been obtained as single crystals from the reaction mixture and characterized by elemental analysis, IR and optical spectroscopy, and single-crystal X-ray diffraction studies. The products are completely insoluble in the most common organic solvents but are freely soluble in water, suggesting the possibility of **1** and **2** existing as ionic compounds. The IR spectra of **1** and **2** are quite similar. A very strong and broad absorption centered at around 3425 cm^{-1} is due to the presence of a large number of coordinated water molecules in **1** and **2**. The phosphoryl absorption in both compounds appears at around 1085 cm^{-1} . The nonobservance of any strong absorption at around 2300 cm^{-1} in the IR spectrum of both **1** and **2** suggests that the dippH_2 ligand is completely deprotonated. The ³¹P NMR spectra of **1** and **2** show single resonances at –4.0 and –3.9 ppm, respectively, with no significant change in the chemical shift values from those observed for free dippH_2 ligand.

Molecular Structures of **1 and **2****. Compound **1** crystallizes in the centrosymmetric monoclinic space group $P2_1/c$ with half of the cation (metal ion on the inversion center), one anion, and two lattice methanol molecules in the asymmetric part of the unit cell. The final refined molecular structure of **1** is shown in Figure 1 along with selected bond lengths. The cationic part of **1** consists of two strontium ions that are surrounded by 14 coordinated water molecules. While four of the water molecules bridge the two metal ions, five water molecules are bound to each metal ion in a terminal fashion. This leads to nine-coordination around each of the strontium ions. The tetrapositive charge of the cationic part is compensated for by the presence of two dipp^{2-} ligands $[(\text{RO})\text{PO}_3^{2-}]$, which do not interact with the metal through the phosphate oxygen atoms. This observation is quite contrary to the earlier reports on group 2 metal phosphonates, where the phosphonate oxygen atoms interact directly with metal ions to produce polymeric layered solids.²² Further, the formation of aqua cationic complexes in the presence of other anionic polyoxo ligands is very common in the case of magnesium, while it is lesser known for heavier group 2 metal ions. Hence, the isolation of **1** and **2**, where only water ligands surround the strontium and barium ions, is a bit surprising.

The four bridging water molecules bring the two strontium ions of **1** close to each other [3.842(1) Å]. This Sr···Sr

- (20) (a) Joyave, J. L.; Steinhauer, L. S.; Dillehay, D. L.; Born, C. K.; Hamrick, M. E. *Biochem. Pharmacol.* **1985**, *34*, 3915. (b) Kunkely, H.; Vogler, A. *Inorg. Chim. Acta* **2004**, *357*, 888. (c) Ranford, J. D.; Sadler, P. J.; Tocher, D. A. *J. Chem. Soc. Dalton Trans.* **1993**, 3393. (d) Brownless, N. J.; Edwards, D. A.; Mahon, M. F. *Inorg. Chim. Acta* **1999**, *287*, 89. (e) In, Y.; Hayashi, C.; Lshida, T. *Inorg. Chim. Acta* **1997**, *260*, 111. (f) Devereux, M.; Curran, M.; McCann, M.; Casey, R. M. T.; Mckee, V. *Polyhedron* **1996**, *15*, 2029. (g) Pavacik, P. S.; Huffman, J. C.; Christou, G. *J. Chem. Soc., Chem. Commun.* **1986**, 43.
- (21) Palanisami, N.; Prabusankar, G.; Murugavel, R. *Inorg. Chem. Commun.* **2006**, *9*, 1002.
- (22) (a) Lima, C. B. A.; Airoidi, C. *Solid State Sci.* **2002**, *4*, 1321. (b) Mahmoudkhani, A. H.; Langer, V. *Solid State Sci.* **2001**, *3*, 519. (c) Svoboda, J.; Zima, V.; Benes, L.; Melanova, K.; Vleck, M. *Inorg. Chem.* **2005**, *44*, 9968. (d) Stone, J. W.; Smith, M. D.; zur Loye, H.-C. *J. Chem. Crystallogr.* **2007**, *37*, 103. (e) Mahmoudkhani, A. H.; Langer, V. *Solid State Sci.* **2001**, *3*, 519. (f) Langley, K. J.; Squattrito, P. J.; Adani, F.; Montoneri, E. *Inorg. Chim. Acta* **1996**, *253*, 77. (g) Cao, G.; Lynch, V. M.; Swinnea, J. S.; Mallouk, T. E. *Inorg. Chem.* **1990**, 2112. (h) Cao, G.; Lee, H.; Lynch, V. M.; Mallouk, T. E. *Solid State Ionics* **1988**, *26*, 63.
- (23) Martin, K. J.; Squattrito, P. J.; Clearfield, A. *Inorg. Chim. Acta* **1989**, *155*, 7.

- (24) Similar reactions involving magnesium and calcium acetate with dippH_2 produced compounds of the formula $[\{\text{Mg}(\text{H}_2\text{O})_6\}\{\text{dipp}\}]$ and $[\{\text{Ca}(\text{H}_2\text{O})_6\}\{\text{dipp}\}]$, for which single-crystal XRD studies could not be carried out because of poor crystal quality.

separation is comparable to that found in $\text{Sr}_2(\mu\text{-dmsO})_3(\text{dmsO})_6(\text{H}_2\text{O})_2 \cdot 2\text{ClO}_4$ (3.84 Å)^{25a} and shorter than those found in $\{[\text{Sr}(\text{2-aminobenzoate})_2(\text{OH})_2 \cdot \text{H}_2\text{O}]\}$ (3.92 Å)^{3a} and $[\text{Sr}_2(\text{tmhd})_4(\text{dmeaH})_2(\mu\text{-dmeaH})_2]$ (4.44 Å) [tmhd = 2,2',6,6'-tetramethylheptane-3,5-dione; dmeaH = (*N,N'*-dimethylamino)ethanol].^{25b} However, this distance is significantly longer than that reported for $[\text{Sr}_2(\text{Q}_6)] \cdot 2\text{ImH}_2$ (3.55 Å) (Q=1-phenyl-3-methyl-4(2,2'-dimethylbutane)(C=O)pyrazol-5-one), where the metal ions are multiply bridged by Q.^{25c}

The Sr–O distances involving the bridging water molecules are somewhat longer [average 2.781(6) Å] compared to the terminal Sr–O distances [average 2.609(5) Å] in **1**. The 36 possible O–Sr–O angles around each of the strontium ions vary over a very wide range [59.3(2)–146.5(2)°]. The polyhedron formed strontium, and the nine water molecules is best described as a monocapped tetragonal antiprism (if a weak metal–metal interaction is also considered, then the coordination environment is a bicapped tetragonal antiprism). In the dipp anion, the dinegative charge is delocalized over the PO_3^{2-} unit, as seen by the nearly equal P–O distances [1.509(7), 1.503(6), and 1.494(6) Å], which are considerably shorter than the P–OAr distance [1.628(6) Å].

The $[\text{Sr}_2(\text{H}_2\text{O})_4]^{4+}$ units, lattice solvent methanol molecules, and the PO_3^{2-} part of the dipp ligands are engaged in extensive O–H···O hydrogen bonding to form a hydrophilic two-dimensional sheet, as shown in Figure 2. There are as many as eight unique hydrogen bonds in **1** whose D···A distances vary from 2.635(8) to 3.192(9) Å; the corresponding D–H···A angles vary in the range 152.9(4)–179.0(8)° (see the Supporting Information). The hydrogen-bonded two-dimensional sheet in **1** is covered by hydrophobic 2,6-diisopropylphenyl groups on either side, thus blocking the propagation of the hydrogen-bonded network to the third

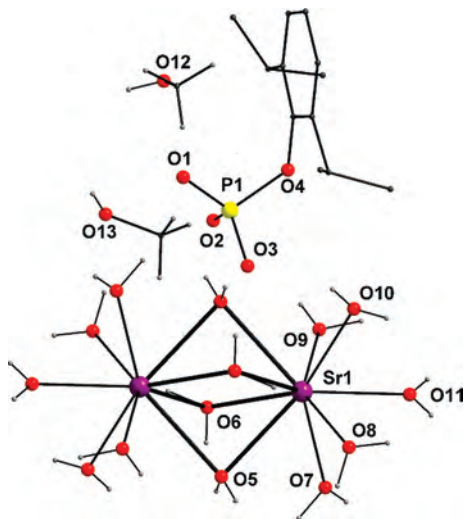


Figure 1. Molecular structure of **1** (one phosphate anion and two lattice methanol solvent molecules are omitted for the sake of clarity). Selected bond distances [Å]: Sr1–O5 2.798(6), Sr1–O5#1 2.826(7), Sr1–O6 2.642(5), Sr1–O6#1 2.859(6), Sr1–O7 2.672(5), Sr1–O8 2.560(7), Sr1–O9 2.693(5), Sr1–O10 2.574(5), Sr1–O11 2.542(4), Sr1···Sr1#1 3.842(1), P1–O1 1.509(7), P1–O2 1.503(6), P1–O3 1.494(6), P1–O4 1.628(5). Symmetry transformations used to generate equivalent atoms: #1, $-x + 1, -y, -z$.

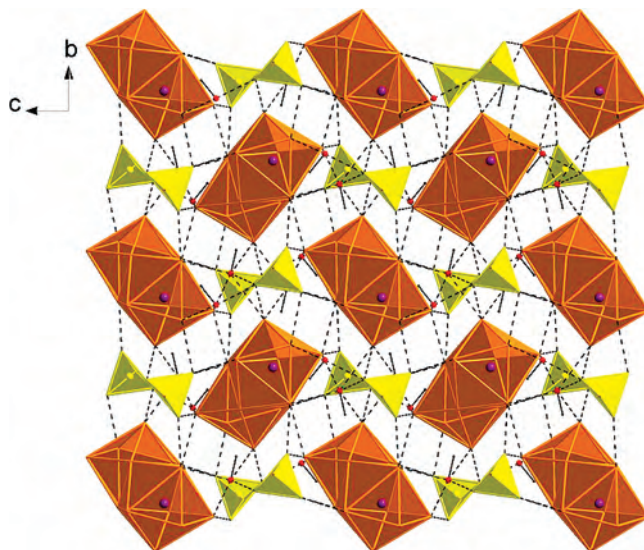


Figure 2. Formation of a hydrogen-bonded sheet structure arising out of the cationic part, PO_3^{2-} part of dipp, and lattice methanol molecules.

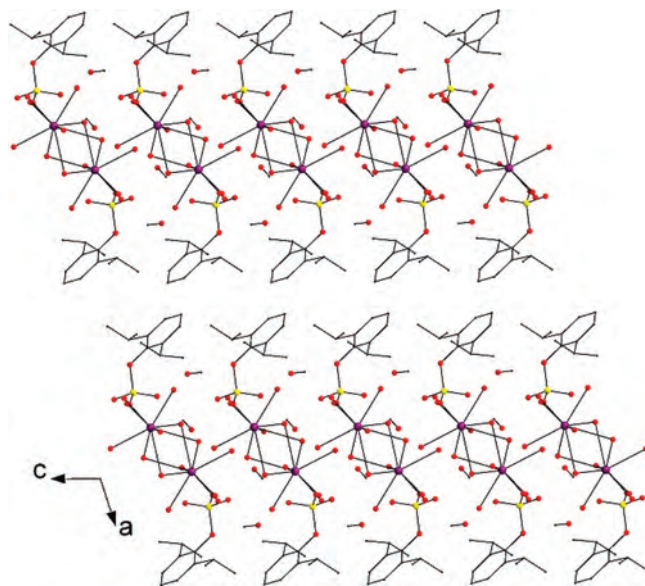


Figure 3. Diagram showing a layered structure in the lattice of **1** (hydrogen atoms omitted for clarity).

dimension. This results in the formation of stacks of the two-dimensional strontium phosphate sheets along the crystallographic *c* axis, as shown in Figure 3. Although this layered structure of **1** somewhat resembles the previously described layered metal phosphonates described for group 2 metal ions,²² the major difference in the present case is the absence of any covalent interaction between the phosphate oxygen and metal ions in **1** (M–O–P linkage).

The molecular structure of **2** is very similar to that of the strontium compound **1** (Figure 4). Although compound **2** also crystallizes in a $P2_1/c$ space group, the asymmetric part contains a full dimeric $\{\text{Ba}_2(\mu\text{-H}_2\text{O})_4(\text{H}_2\text{O})_{10}\}$ unit along with two dipp anions. Additionally, in **2**, four lattice water molecules replace the four methanol lattice solvents found for **1**. Other structural features of **2** are quite similar to that described above for **1**. The two barium ions, which are bridged by four water molecules, are separated from each other by 4.049(1) Å. This distance is somewhat longer than

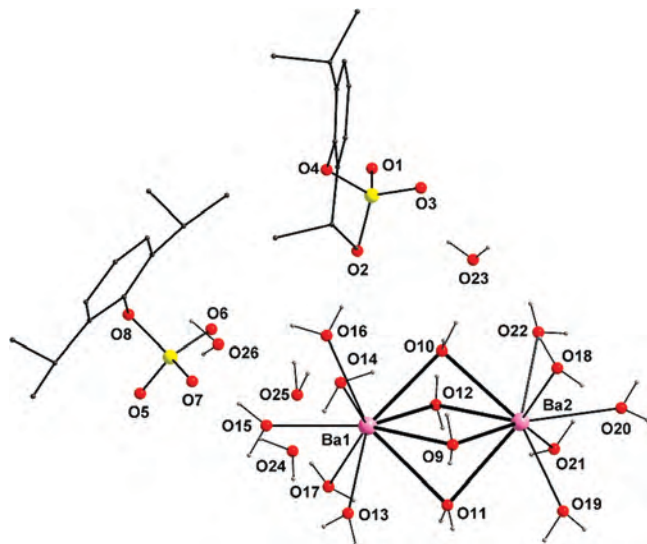


Figure 4. Molecular structure of **2**. Selected bond distances [Å]: Ba1–O9 2.982(5), Ba1–O10 2.875(5), Ba1–O11 3.063(5), Ba1–O12 2.815(5), Ba1–O13 2.777(5), Ba1–O14 2.756(5), Ba1–O15 2.681(5), Ba1–O16 2.933(5), Ba1–O17 2.891(5), Ba2–O9 2.809(5), Ba2–O10 2.928(5), Ba2–O11 2.975(5), Ba2–O12 2.962(5), Ba2–O18 2.837(5), Ba2–O19 2.851(5), Ba2–O20 2.708(5), Ba2–O21 2.764(6), Ba2–O22 2.678(5), Ba1···Ba2 4.0486(6), P1–O1 1.522(5), P1–O2 1.520(5), P1–O3 1.533(5), P1–O4 1.633(4), P2–O5 1.523(5), P2–O6 1.536(5), P2–O7 1.523(5), P2–O8 1.635(5).

that found for $\text{Ba}_2(\mu\text{-dmsO})_4(\text{dmsO})_6(\text{H}_2\text{O})_2 \cdot (\text{ClO}_4)_2$ (3.94 Å)^{25a} but is considerably shorter than that observed for polymeric $[\text{Ba}(\text{2-aminobenzoate})_2(\text{OH}_2)]_n$ (4.32 Å).^{3a}

The Ba–O distances associated with the bridging water molecules are significantly longer [range: 2.809(5)–3.063 Å; average 2.926(5) Å] compared to the Ba–O distances involving terminal water molecules [range: 2.678(5)–2.933 Å; average 2.788(5) Å]. The O–Ba–O angles in **2** vary over a wide range [57.3(1)–147.4(1)° for Ba1 and 58.6(1)–146.3(2)° for Ba2] because of the coordination number of 9 around the barium ions. As in the case of **1**, the polyhedron formed by barium and the nine water molecules is a monocapped tetragonal antiprism. In both of the dipp anions, there is a charge delocalization over the entire PO_3 unit as revealed by the nearly equal P–O distances [1.520(5), 1.522(5), and 1.533(5) Å for P1 and 1.523(5), 1.523(5), and 1.536(6) Å for P2], which are considerably shorter than the P–OAr distances [1.633(5) and 1.635(5) Å].

The supramolecular aggregation that has been observed for **2** is very similar to **1**, although the presence of lattice water molecules (in place of methanol in **1**) produces a much more extensive hydrogen-bonded network of the hydrophilic units of the compound. In fact, a total of 27 unique O–H···O hydrogen bonds have been observed in **2** (see the Supporting Information). The D···A distances of these interactions vary from 2.664(8) to 3.228(8) Å, while the corresponding D–H···A angles fall in the range 142.8(4)–176.5(3)° (see the Supporting Information). Except for the large number of hydrogen bonds found in **2**, the supramolecular aggregation behavior in both **1** and **2** is very similar, as can be seen from the layered structure depicted for **2** in Figure 5.

Synthesis of 3–6. Intrigued by the absence of direct metal to phosphate coordination in both **1** and **2**, we turned our

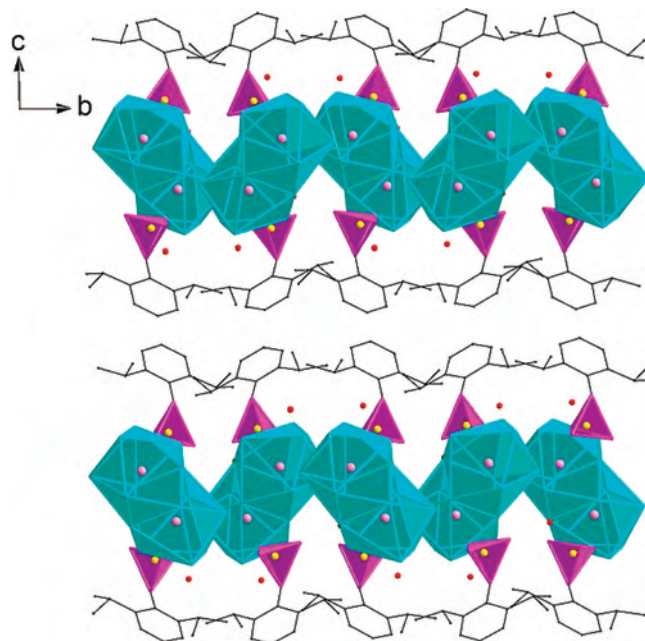
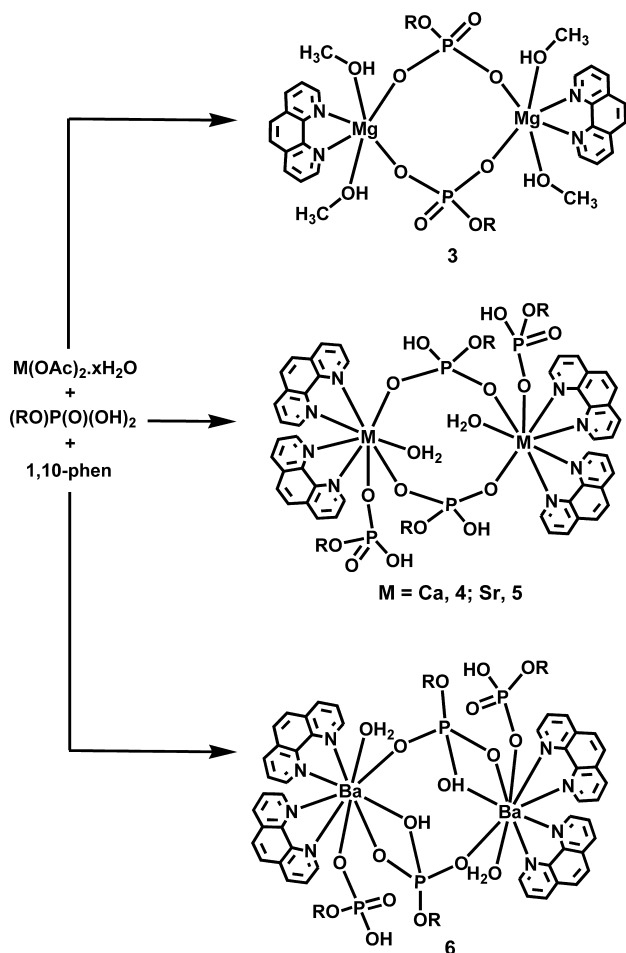


Figure 5. Layered structure of **2** (hydrogen atoms omitted for clarity).

attention to finding ways to isolate group 2 metal phosphates with direct M–O–P linkages. In a very recent study, we have unraveled the so-called softer side of group 2 metal ions by synthesizing a series of alkaline-earth metal salicylate and anthranilate complexes in the presence of pyridinic ligands.^{3a,4a} Interestingly, when 1,10-phenanthroline was used, the simultaneous incorporation of both carboxylate and phen ligands in to the metal coordination sphere was observed. On the other hand, when 4,4'-bipyridine was used, only metal carboxylate complexes with lattice bpy molecules were isolated. This study led to the conclusion that only chelating nitrogen-donor ligands can be incorporated into the coordination sphere of group 2 cations.

Thus, the use of phen in the reactions of group 2 metal ions with dippH₂ not only opens up a greater chance of replacing some of the water ligands from the metal but can also bring the dipp ligand (due to the hydrophobicity of the metal-bound phen ligand) to the coordination sphere of the metal. To validate such a cooperative binding of both phen and dipp to group 2 ions, the synthesis of alkaline-earth metal phosphate complexes $[\text{M}(\text{phen})(\text{dipp})(\text{CH}_3\text{OH})_2]_2$ (**3**) and $[\text{M}(\text{phen})_2(\text{dippH})_2(\text{H}_2\text{O})]_2$ [$\text{M} = \text{Ca}$ (**4**), Sr (**5**), Ba (**6**)] was accomplished by the reaction of $\text{M}(\text{OAc})_2 \cdot x\text{H}_2\text{O}$ ($\text{M} = \text{Mg}$, Ca , Sr , Ba) and dippH₂ in the presence of phen as the auxiliary ligand in an aqueous methanolic solution (Scheme 2). X-ray-quality single crystals of air-stable **3–6** were obtained in high yields by slow evaporation of the solvent under ambient conditions. The analytically pure complexes **3–6** were characterized by means of IR spectroscopy, elemental analysis, DRUV–vis spectroscopy, fluorescence emission spectroscopy, and thermogravimetric analysis (TGA) under a dinitrogen atmosphere. Furthermore, the molecular structures of all complexes have been established by single-crystal X-ray diffraction (XRD) analyses.

IR Spectra and DRUV–Vis. In the IR spectrum of **3**, no P–OH stretching frequency appears in the range of 2350

Scheme 2. Synthesis of Dimeric Alkaline-Earth Metal Phosphate Complexes 3–6

cm^{-1} , confirming the complete deprotonation of the dippH_2 . However, a broad absorption band is observed in the IR spectra of 4–6 at 2324 (4), 2406 (5), and 2350 cm^{-1} (6), respectively, indicating incomplete neutralization of dippH_2 ²⁶ in these complexes. For all new compounds, strong absorption bands in the range of 1100–990 cm^{-1} are observed for the phosphate metal bonds (MO–P asymmetric and symmetric stretching frequency) with slightly smaller wavenumbers for the heavier 4–6 (due to the longer MO–P bond distances *vide infra*). The DRUV–vis spectra of 3–6 show an absorption in the broad range of 265 and 330 nm and an emission in the range of 420 nm. The strong emission of 3–6 arises presumably from ligand-to-metal charge transfer.

Molecular Structures of 3–6. In order to understand the influence of the auxiliary phen ligand and to compare the structural changes upon variation of the alkaline-earth metal center, a detailed single-crystal X-ray structural investigation has been carried out. Because the solution structure differs significantly from the solid-state structure in the case of group 2 metal complexes,^{3,4} this structural study is essential for

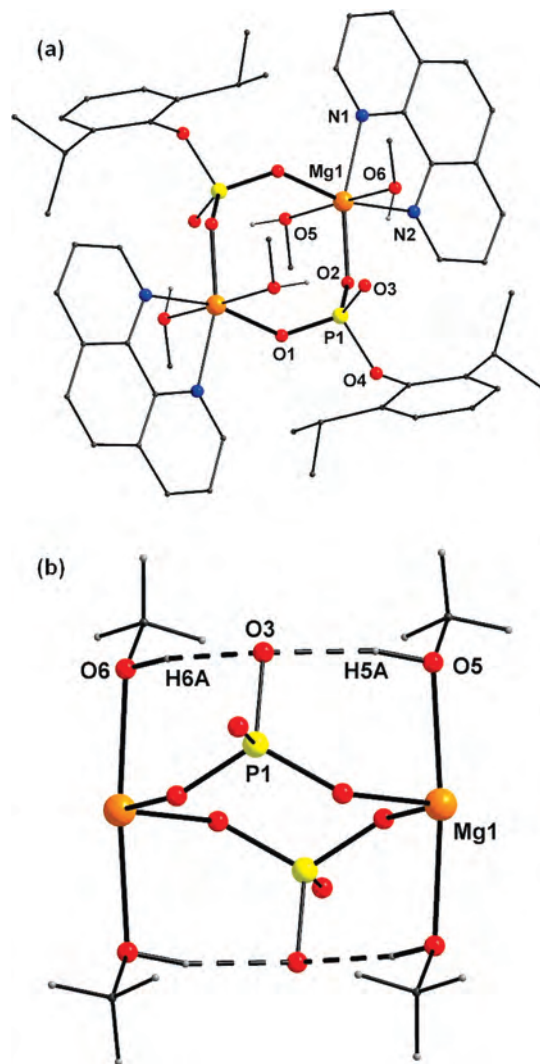


Figure 6. (top) Molecular structure of 3 (lattice methanol and hydrogen atoms omitted for the sake of clarity) and (bottom) core structure of 3 showing intramolecular hydrogen bonding. Selected bond distances [Å]: Mg1–N1 2.229(2), Mg1–N2 2.218(1), Mg1–O1 1.980(1), Mg1–O2#1 1.992(1), Mg1–O5 2.140(1), Mg1–O6 2.126(1), P1–O1 1.502(1), P1–O2 1.506(1), P1–O3 1.529(1), P1–O4 1.629(1). Selected bond angles [deg]: N1–Mg1–N2 74.30(5), N1–Mg1–O1 89.41(5), N1–Mg1–O2#1 163.92(5), N1–Mg1–O5 93.32(5), N1–Mg1–O6 90.78(5), N2–Mg1–O1 162.77(5), N2–Mg1–O2#1 90.32(5), N2–Mg1–O5 89.77(5), N2–Mg1–O6 95.05(5), O1–Mg1–O2#1 106.33(5), O1–Mg1–O5 85.55(5), O1–Mg1–O6 90.65(5), O2#1–Mg1–O5 91.23(5), O2#1–Mg1–O6 85.86(5), O5–Mg1–O6 174.38(5). Symmetry transformations used to generate equivalent atoms: #1, $-x, -y, -z$.

the understanding of the chemical behavior of the complexes 3–6. Selected bond lengths and angles for each compound are listed in the respective figure captions.

The dimeric magnesium complex 3 is composed of two magnesium atoms and two phosphate moieties with four bridging μ -oxygen atoms forming a central eight-membered $\text{Mg}_2\text{O}_4\text{P}_2$ ring (Figure 6a). Each octahedral magnesium atom is bound to a chelating phenanthroline molecule and two phosphate oxygen atoms in the equatorial and to two methanol molecules in the axial positions. The average Mg–O(phos), Mg–O(CH_3OH), and Mg–N distances (1.986, 2.133, and 2.223 Å, respectively) are comparable with the corresponding distances found in known magnesium/zinc

(25) (a) Harrowfield, J. M.; Richmond, W. R.; Skelton, B. W.; White, A. H. *Eur. J. Inorg. Chem.* **2004**, 227. (b) Davies, H. O.; Brooks, J. J.; Jones, A. C.; Leedham, T. J.; Bickley, J. F.; Steiner, A.; O'Brien, P.; White, A. J. P.; Williams, D. J. *Polyhedron* **2001**, *20*, 2397. (c) Marchetti, F.; Pettinari, C.; Pettinari, R.; Cingolani, A.; Drozdov, A.; Troyanov, S. *J. Chem. Soc., Dalton Trans.* **2002**, 2616.

(26) $\nu(\text{PO}-\text{H})$ for $\text{dippH}_2 = 2385 \text{ cm}^{-1}$.

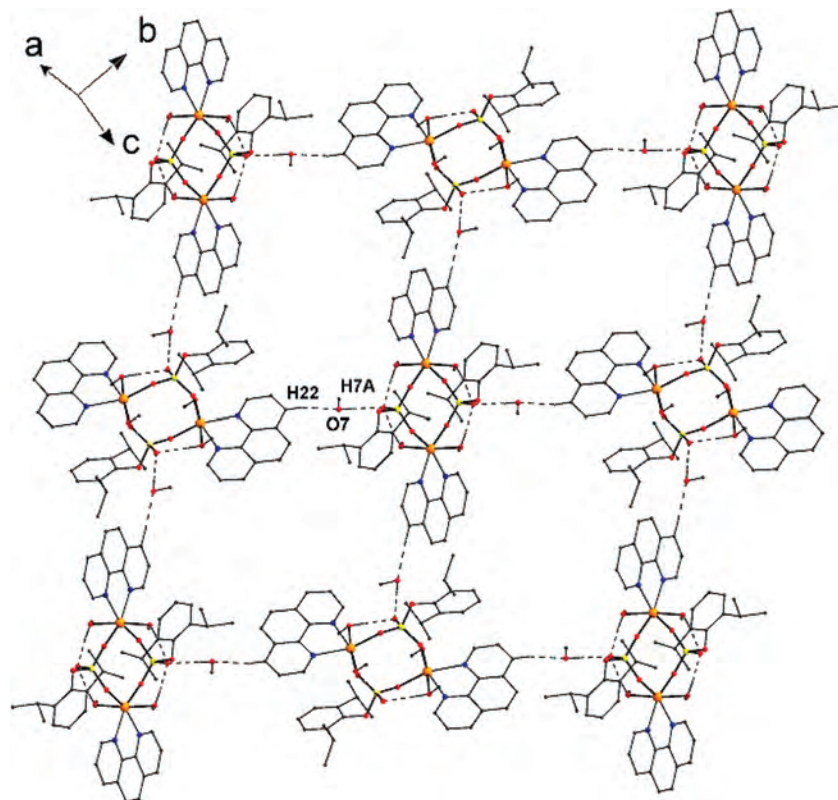


Figure 7. Rectangular grid formation in **3** through intermolecular hydrogen-bonding interactions.

phosphates or phosphonates in the literature.^{13,27} Because the phosphates coordinate via two of the oxygen atoms, charge delocalization is observed within this moiety and thus no formal P–O and P=O bonds are found. The observed P–O bond distances [P1–O1 1.502(1) Å, P1–O2 1.506(1) Å, and P1–O3 1.529(1) Å] are considerably shorter than a formal P–O bond (1.59–1.60 Å) but significantly longer than a formal P=O bond (1.45–1.46 Å).³⁰ The central eight-membered ring is involved in two intramolecular hydrogen bonds [O5–H5A···O3 2.697(1) Å, 165.23(8)°; O6–H6A···O3 2.712(1) Å, angle], arising between the coordinated methanol O–H group and the phosphoryl oxygen atoms and, thus, a twelve-membered, an eight-membered, and four six-membered rings are formed in the dimeric unit (broken bonds in Figure 6b). In addition, the uncoordinated methanol molecules and the aromatic C–H groups bridge the magnesium phosphate dimers by intermolecular hydrogen bonds [C22–H22···O7 3.268(2) Å, 148.7(1)°; O7–H7A···O3 2.715(2) Å, 174.4(1)°] and result in the formation of an infinite two-dimensional grid structure (Figure 7).

The increase of the ionic radius brings along significant structural changes in the case of calcium and strontium derivatives **4** and **5**. Compounds **4** and **5** are isostructural. The *Diamond* presentations²⁸ of the molecular structures of **4** and **5** are depicted in Figure 8. The increased inner-coordination sphere in complexes **4** and **5** allows the bonding of two phenanthroline molecules, two bridging monoanionic phosphate moieties (dippH), one monodentate phosphate anion, and one water, thus leading to eight-coordinated metal centers. As in **3**, the phosphate ligands are bridging with two oxygen atoms between two alkaline-earth metal centers, resulting in the formation of a dimer with a nonplanar M₂O₄P₂ ring in the core. The M–O and M–N bonds in **4** and **5** fall in the expected range and are comparable with corresponding carboxylate and phosphate/phosphonate complexes.²² The hydrogen atoms of the coordinated water molecules undergo a strong interaction with phosphoryl oxygen atoms as well as the P–OH protons bound to the phosphate oxygen atoms. In compound **4**, the intramolecular hydrogen-bond contacts O3–H3A···O7 [2.486(2) Å; 167.2(1)°], O6–H6A···O2 [2.617(1) Å; 169.9(1)°], and O9–H9A···O3 [2.867(2) Å; 166.4(1)°] are found. As a result, a cage-like structure is observed for the inner-coordination sphere of **4** and **5** (Figure 9). Weak interactions between phenanthroline C–H hydrogen atoms and the phosphate oxygens [C30–H30···O8 3.447(3) Å, 176.78(2)°, in **4**; 3.492(2) Å, 176.9(1)°, in **5**] bring about a supramolecular aggregation in the form of a one-dimensional chain, as shown in Figure 10.²⁹

Additional structural changes are observed for the barium complex **6** (Figure 11) compared to the above-described calcium and strontium derivatives in spite of the fact that all three compounds have the same molecular formula,

- (27) (a) Weis, K.; Rombach, M.; Vahrenkamp, H. *Inorg. Chem.* **1998**, *37*, 2470. (b) Fry, F. H.; Jensen, P.; Kepert, C. M.; Spiccia, L. *Inorg. Chem.* **2003**, *42*, 5637. (c) Mao, B. G.; Clearfield, A. *Inorg. Chem.* **2002**, *41*, 2319. (d) Onoda, A.; Yamada, Y.; Okamura, T.; Doi, M.; Yamamoto, H.; Ueyama, N. *J. Am. Chem. Soc.* **2002**, *124*, 1052. (e) Kontturi, M.; Peraniemi, S.; Vepsäläinen, J. J.; Ahlgren, M. *Polyhedron* **2005**, *24*, 305. (f) Hursthouse, M. B.; Levason, W.; Ratnani, R.; Reid, G.; Stainer, H.; Webster, M. *Polyhedron* **2005**, *24*, 121. (g) Lutz, M.; Müller, G. *Inorg. Chim. Acta* **1995**, *232*, 189.
- (28) *Diamond*, version 2.10; Crystal Impact GbR: Bonn, Germany, 2001.
- (29) (a) Desiraju, G. R. *Acc. Chem. Res.* **1996**, *29*, 441. (b) Desiraju, G. R. *Acc. Chem. Res.* **1991**, *24*, 290.
- (30) Bauer, S.; Müller, H.; Bein, T.; Stock, N. *Inorg. Chem.* **2005**, *44*, 9464.

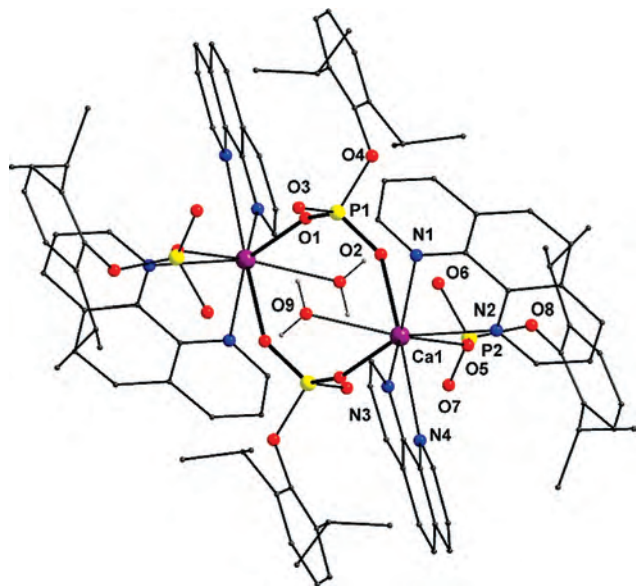


Figure 8. Molecular structure of **4** (and isostructural **5**) (hydrogen atoms omitted for the sake of clarity). Selected bond distances [Å] for **4**: Ca1–N1 2.693(2), Ca1–N2 2.618(2), Ca1–N3 2.698(2), Ca1–N4 2.599(2), Ca1–O1 2.391(2), Ca1–O2 2.466(2), Ca1–O5 2.337(2), Ca1–O9 2.479(2), P1–O1#1 1.483(2), P1–O2 1.502(2), P1–O3 1.566(2), P1–O4 1.618(2), P2–O5 1.484(2), P2–O6 1.572(2), P2–O7 1.504(2), P2–O8 1.606(2). Selected bond distances [Å] for **5**: Sr1–N1 2.799(2), Sr1–N2 2.728(2), Sr1–N3 2.792(2), Sr1–N4 2.709(2), Sr1–O1 2.496(2), Sr1–O2 2.578(2), Sr1–O5 2.475(2), Sr1–O9 2.607(2), P1–O1#1 1.480(2), P1–O2 1.500(2), P1–O3 1.571(2), P1–O4 1.621(2), P2–O5 1.478(2), P2–O6 1.505(2), P2–O7 1.574(2), P2–O8 1.608(2). Symmetry transformations used to generate equivalent atoms: #1, $-x + 1, -y + 1, -z$.

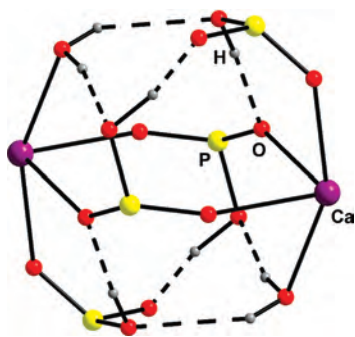


Figure 9. Cage formation in **4** through strong intramolecular hydrogen-bonding interactions.

$[M(\text{dippH})_2(\text{phen})_2(\text{H}_2\text{O})_2]$. As in the case of **5**, two phenanthroline molecules and two phosphate moieties are coordinated to the two barium ions, although the mode of phosphate binding is different in this case. The un-ionized P–OH group also takes part in the metal coordination in the present case. The hydroxyl oxygen atom of the bridging phosphate binds weakly to the central metal atom, resulting in a nine-coordinated Ba^{2+} center. Thus, the bridging phosphate ligand now also chelates one of the two metals. The bridging mode of coordination exhibited by dipp in **6** is unprecedented in metal phosphate monoester complexes and is also unknown in the metal di-*tert*-butylphosphate chemistry investigated by us some years ago.¹⁷

The core of the dimeric **6**, which is a $\text{Ba}_2\text{P}_4\text{O}_{12}$ aggregate, resembles that of an open cubane (Figure 12). While coordinated water hydroxyl protons undergo just a weak interaction [$\text{O9–H9A}\cdots\text{O13}$ 2.791(7) Å, 175(8)°], the

undissociated hydroxyl protons of phosphate moieties interact strongly with phosphoryl oxygen atoms. The hydrogen bonds $\text{O3–H3A}\cdots\text{O6}$ and $\text{O7–H7A}\cdots\text{O2}$ are observed with $\text{D}\cdots\text{A}$ distances of 2.520(4) and 2.539(4) Å, respectively, and the $\text{D–H}\cdots\text{A}$ angles are close to linearity [168(6)° and 174(5)°]. The Ba–O and Ba–N distances are comparable to those of barium carboxylate and phosphate/phosphonates, which contain additional nitrogen-donor ligands.³⁰ Weak hydrogen bonds between phenanthroline hydrogen atoms and aryl-substituted oxygens [$\text{C43–H43}\cdots\text{O4}$ 3.372(4) Å, 177.6(2)°] result in a two-dimensional gridlike arrangement (Figure 13), which somewhat resembles the aggregation in **3**.

Comparison of the X-ray Structures 3–6. A comparison of key structural parameters of dimeric phosphates **3–6** along with those of the ionic phosphates **1** and **2** is presented in Table 1. Because the literature on group 2 metal phosphate complexes is very sparse and the dinuclear metal phosphate complexes are unknown for group 2 metal ions, no efforts have been made to compare the data presented in Table 1 with those of any literature examples. As can be seen from Table 1 and Figure 14, all dinuclear compounds are built around a $\text{M}_2\text{O}_4\text{P}_2$ ring whose conformation changes considerably in passing from **3** to **6**. The eight-membered ring exists in a staircaselike conformation for **3** (Figure 14) because of similar M–O and P–O distances within the ring. The increase in the M–O distances without any corresponding change in the P–O distances in the case of **4** and **5** results in a ring conformation in which six of the eight ring atoms lie in a plane; the other two atoms (O2 and O2') occupy positions above and below this plane, as shown in Figure 14. The ring conformation in the case of barium derivative **6** is similar to that of **4** and **5** but for the additional phosphate oxygen binding (O3 and O3') to the barium ions, as depicted in Figure 14, to produce the two BaO_2P four-membered rings within the molecular core (vide supra).

Interesting among the data presented in Table 1 is the coordination mode exhibited by the dipp ligand in these complexes. While dipp does not bind to metal in **1** and **2**, three different coordination modes are found for the dipp ligands in the dimeric compounds **3–6**. The bridging dipp ligand in **3–5** binds in a [2.110] mode (Harris notation)³¹ with one of the phosphoryl oxygen atoms not involved in metal binding. However, a [3.111] binding mode is observed for the bridging dipp in the barium derivative **6** because of its ability to chelate one of the barium ions apart from bridging the other, probably owing to the larger ionic radius of barium and the larger Ba–O(P) distances. The terminal phosphate ligands in **4–6** exhibit a [1.100] binding mode. The $\text{M}\cdots\text{M}$ distances in these systems again follow a trend. The quadruply aqua-bridged strontium and barium compounds **1** and **2** show the shortest nonbonded metal separation among the present compounds (Table 1). The steady increase in $\text{M}\cdots\text{M}$ for compounds **3** and **4** is consistent with the corresponding increase in the ionic distance. The reduction in $\text{M}\cdots\text{M}$ for **6** could, however, be explained by the formation of two four-membered chelate rings around the

(31) Coxall, R. A.; Harris, S. G.; Henderson, D. K.; Parsons, S.; Tasker, P. A.; Winpenny, R. E. P. *J. Chem. Soc., Dalton Trans.* **2000**, 2349.

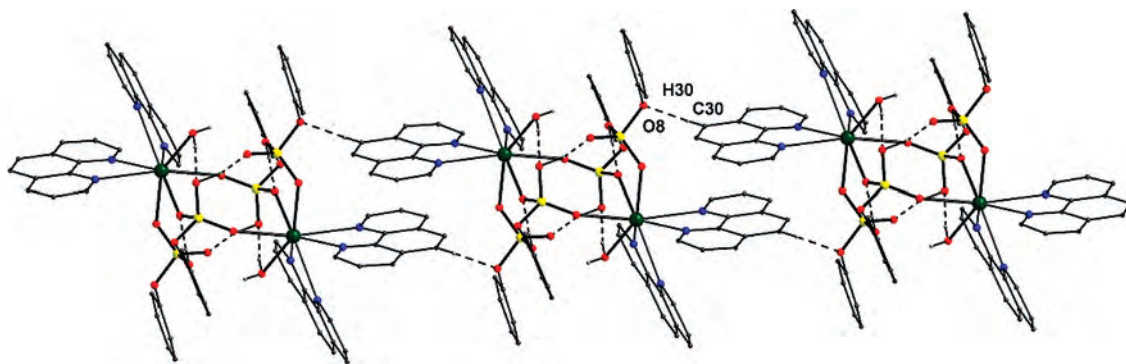


Figure 10. One-dimensional polymeric chain formation in **4** and **5** via C–H···O interactions.

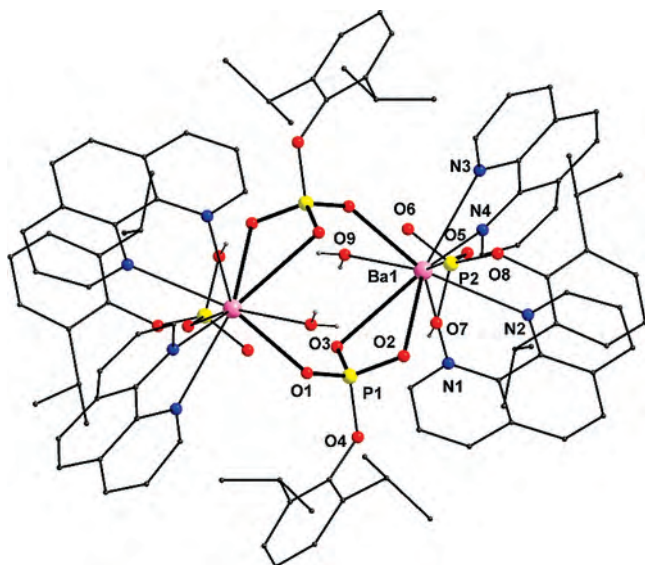


Figure 11. Molecular structure of **6** (lattice methanol, water molecules, and hydrogen atoms omitted for the sake of clarity). Selected bond distances [Å]: Ba1–N1 2.965(3), Ba1–N2 2.920(3), Ba1–N3 2.933(3), Ba1–N4 2.985(3), Ba1–O1 2.692(2), Ba1–O2 2.887(2), Ba1–O3 2.940(2), Ba1–O5 2.735(2), Ba1–O9 2.870(3), P1#1–O1 1.490(2), P1–O2 1.513(2), P1–O3 1.576(3), P1–O4 1.624(2), P2–O5 1.489(2), P2–O6 1.510(2), P2–O7 1.574(3), P2–O8 1.623(2). Symmetry transformations used to generate equivalent atoms: #1, $-x + 1, -y + 2, -z + 2$.

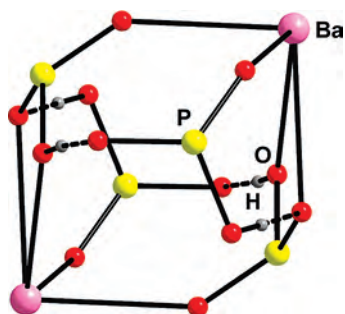


Figure 12. Strong intramolecular hydrogen-bonding interactions assisted the cubanelike cage formation in the core of **6**.

barium ions, which makes a smaller angle at O3; as a consequence, the barium ions in **6** move a little close to each other compared to the strontium ions in **5**.

The presence of P=O, P–OH, and C–H groups along with coordinated and lattice solvent molecules produces a large number of intramolecular and few intermolecular hydrogen bonds in each case, which leads to an interesting supramolecular aggregation of the individual molecules in

the crystal lattice. Depending on the position and relative orientation of these potential hydrogen-bonding sites, either a one-dimensional polymer or a two-dimensional sheet are observed for compounds **3–6**, whereas in the case of ionic phosphates **1** and **2**, a layered structure is obtained (Table 1).

Thermal Decomposition Studies. Because of the interest in ceramic phosphates of group 2 metal ions for various applications and the interest in biomineralization of calcium phosphate structures, the thermal behavior of all of the new compounds has been investigated by TGA/DTA/DSC analysis. The TGA of all of the compounds underwent elimination of coordinated solvent molecules and thermal decomposition of all volatile organic residues in a stepwise manner (details are given in the Supporting Information) to produce the ceramic phosphates. In order to identify the phases formed at the end of decomposition, a parallel bulk thermolysis was carried for all compounds in air at 600 °C for 8 h and the decomposition product was further examined by powder XRD (PXRD). Compounds **1** and **2** decompose cleanly to the metal pyrophosphate, $M_2P_2O_7$ ($M = Sr, Ba$), as identified by a comparison of the PXRD of the decomposition product with that of an authentic sample reported in JCPDS.³² On the other hand, compounds **4–6** produce the metaphosphates $M(PO_3)_2$ ($M = Ca, Sr, Ba$) with no detectable amounts of the pyrophosphates in the PXRD of the products. The formation of pyrophosphate for one set of compounds and the metaphosphate for the other set is consistent with the fact that the ratio of metal ion to dipp ligand in the case of complexes **1** and **2** is 1:1, and in the case of dimers **4–6**, the ratio is 1:2. The removal of P_2O_5 to form the pyrophosphate was not observed up to 800 °C during the decomposition of **4–6**.

Conclusion

We have shown in this contribution that the synthesis of alkaline-earth metal phosphates can be achieved under mild conditions in either the presence or absence of the chelating nitrogen-donor phenanthroline. The surprising outcome of these studies is that, even for larger strontium and barium

(32) (a) McIntosh, A. O.; Jablonski, W. L. *Anal. Chem.* **1956**, *28*, 1424. (b) Ropp, R.; Aia, M. A.; Hoffmann, C. W. W.; Veleker, T. J.; Mooney, R. W. *Anal. Chem.* **1959**, *31*, 1163. (c) Grenier, J. C.; Masse, R. *Bull. Soc. Fr. Mineral. Cristallogr.* **1967**, *90*, 285. (d) El Belghitti, A. A.; Elmarzouki, A.; Boukhari, A.; Holt, E. M. *Acta Crystallogr., Sect. C* **1995**, *51*, 1478. (e) Hoffmann, C. W. W.; Mooney, R. W. *J. Electrochem. Soc.* **1960**, *107*, 854.

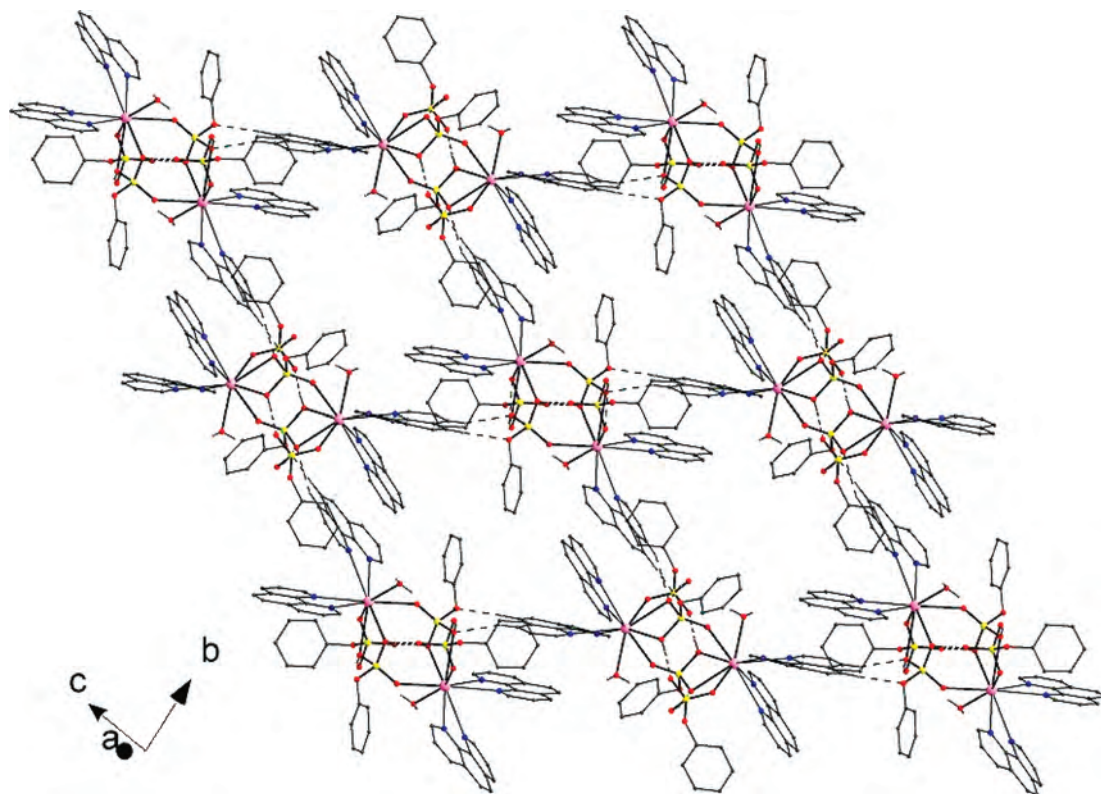


Figure 13. Intermolecular hydrogen-bonding interactions in **6** leading to a rectangular grid.

Table 1. Comparison of Structural Parameters in Group 2 Metal Phosphates **1–6**

compound	basic structure	hydrogen-bonded aggregation	metal coordination number; geometry	phosphate binding ³¹	M···M, Å	P···P, Å
1	ionic	layered	9; monocapped tetragonal antiprism		3.842(1)	
2	ionic	layered	9; monocapped tetragonal antiprism		4.0486(6)	
3	dimer	2D grid	6; octahedral	[2.110]	4.922(1)	4.177(2)
4	dimer	1D polymer	8; distorted bicapped octahedron	[2.110], [1.100]	6.192(5)	4.366(1)
5	dimer	1D polymer	8; distorted bicapped octahedron	[2.110], [1.100]	6.305(5)	4.531(1)
6	dimer	2D grid	9; highly irregular	[3.111], [1.100]	6.052(23)	4.579(4)

ions, in the absence of nitrogen donor, simple aqua-ligand-coordinated complexes are isolated, whereas similar reactions with phosphonic acids yield highly covalent polymeric solids.²² The introduction of a nitrogen donor, however, produces cooperativity in simultaneous dipp and nitrogen-donor binding, to yield a series of structurally diverse dinuclear group 2 phosphates **3–6**. To our knowledge, these are the first examples of group 2 metal phosphates in the literature where the metal ion also binds to a soft pyridinic nitrogen-donor ligand. In the case of barium compound **6**, for the first time, a chelating mode of coordination has been observed for the monoester phosphate ligand. In addition to

bringing cooperativity, the bidentate phen also prevents by coordination expansion to polymeric frameworks. Clearly, the two types of reactions investigated in the present study have opened up further possibilities in the phosphate chemistry of group 2 metal ions. The investigation of reactions of dippH₂ with organometallic group 2 precursors in anaerobic conditions in the presence of other donor solvents could lead to more interesting metal phosphate clusters with no aqua ligands. We are currently investigating these aspects.

Experimental Section

Apparatus. IR spectra were obtained from a Nicolet Impact-400 FTIR spectrometer. The melting points were measured in glass capillaries and were reported to be uncorrected. Microanalyses were performed on a Thermo Finnigan (FLASH EA 1112) or a Carlo Erba 1106 microanalyzer. TGA was carried out on a Perkin-Elmer thermal analysis system, under a stream of nitrogen gas. Collections of PXRD data were obtained with a Philips X'Pert Pro X-ray diffraction system using monochromated Cu K α radiation ($\lambda = 1.5406$ Å). UV–vis spectra were obtained on a Shimadzu UV-260 spectrophotometer, and the fluorescence was recorded on a Perkin-Elmer LS-55 Luminescence spectrometer.

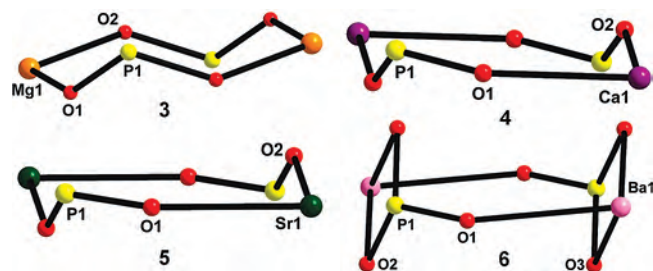


Figure 14. Conformation of the centrosymmetric M₂P₂O₄ eight-membered rings in **3–6**.

Table 2. Crystal Data and Structure Refinement for 1–6

compound	1	2	3	4	5	6
formula	C ₂₈ H ₇₈ O ₂₆ P ₂ Sr ₂	C ₂₄ H ₇₀ Ba ₂ O ₂₆ P ₂	C ₅₄ H ₇₄ Mg ₂ N ₄ O ₁₄ P ₂	C ₉₆ H ₁₀₈ Ca ₂ N ₈ O ₁₈ P ₄	C ₉₆ H ₁₀₈ N ₈ O ₁₈ P ₄ Sr ₂	C ₁₀₂ H ₁₃₆ Ba ₂ N ₈ O ₂₆ P ₄
fw	1068.08	1111.42	1113.74	1865.94	1961.02	2288.75
temp, K	150(2)	150(2)	120(2)	150(2)	133(2)	133(2)
cryst syst	monoclinic	monoclinic	monoclinic	monoclinic	monoclinic	monoclinic
Space group	<i>P</i> ₂ ₁ / <i>c</i>	<i>P</i> ₂ ₁ / <i>c</i>	<i>P</i> ₂ ₁ / <i>n</i>	<i>P</i> ₂ ₁ / <i>n</i>	<i>P</i> ₂ ₁ / <i>n</i>	<i>P</i> ₂ ₁ / <i>n</i>
<i>a</i> , Å	18.0616(13)	12.1326(5)	11.3546(4)	13.5565(3)	13.6801(3)	15.062 (1)
<i>b</i> , Å	10.7103(7)	10.9146(6)	23.7094(6)	16.4318(3)	16.4962(4)	15.382(1)
<i>c</i> , Å	11.8239(10)	34.4456(15)	12.0419(4)	21.6158(4)	21.7229(5)	24.072(2)
β, deg	107.532(7)	91.437(4)	116.096(4)	100.874(2)	99.663(2)	105.720(8)
<i>V</i> , Å ³	4862.4(5)	4559.9(4)	2911.3(2)	4728.6(2)	4832.7(2)	5368.3(6)
<i>Z</i>	2	4	2	2	2	2
<i>D</i> (calcd), g/cm ³	1.626	1.619	1.270	1.311	1.348	1.416
μ, mm ⁻¹	2.608	1.867	0.161	0.259	1.240	0.864
cryst size, mm ³	0.33 × 0.26 × 0.19	0.27 × 0.25 × 0.22	0.36 × 0.29 × 0.22	0.26 × 0.22 × 0.19	0.26 × 0.21 × 0.18	0.35 × 0.32 × 0.29
θ range, deg	3.04–25.00	2.94–25.00	3.19–32.56	2.91–25.00	2.97–25.00	2.95–25.00
no. of reflns collected	11 283	33 609	19 904	40 805	37 199	29 369
no. of obsd reflns	3754	8018	5133	8309	8462	9390
[<i>I</i> ₀ > 2σ(<i>I</i> ₀)]						
GOF	1.087	1.205	1.233	1.073	1.071	1.072
R1 [<i>I</i> ₀ > 2σ(<i>I</i> ₀)]	0.0688	0.0594	0.0338	0.0429	0.0289	0.0363
wR2 (all data)	0.2035	0.1304	0.1022	0.0959	0.0796	0.0848
largest hole and peak, e Å ⁻³	−1.703 and 1.959	−1.292 and 2.738	−0.337 and 0.327	−0.443 and 0.788	−0.383 and 0.544	−0.687 and 0.875

Materials. Commercial-grade solvents were purified by employing conventional procedures and were distilled prior use. Commercially available starting materials such as 1,10-phenanthroline monohydrate (S. D. Fine Chemicals), Mg(OAc)₂·4H₂O (S. D. Fine Chemicals), Ca(OAc)₂ (British drug house, India), Sr(OAc)₂ (Aldrich), and Ba(OAc)₂ (S. D. Fine Chemicals) were used as received. Diisopropylphenyl phosphate was synthesized as described previously in the literature.³³

Synthesis of [(M₂(μ-H₂O)₄(H₂O)₁₀){dipp}₂]₂·4L [M = Sr, L = CH₃OH (1); M = Ba, L = H₂O (2)]. A solution of dippH₂ (258 mg, 1 mmol) in methanol (10 mL) was added to the solution CH₃OH/H₂O (30/5 mL) of Sr(OAc)₂ (205 mg, 1 mmol)/Ba(OAc)₂ (255 mg, 1 mmol). The resulting solution was stirred at room temperature to obtain a clear solution and filtered using filter paper. Colorless single crystals of **1** or **2** were obtained from the filtrate after 5–6 days by slow evaporation of the solvent.

1. Mp: >275 °C. Yield: 0.32 g (60%). Anal. Calcd for C₁₄H₃₉O₁₃PSr (*M*_r = 534.05): C, 31.49; H, 7.36. Found: C, 29.49; H, 6.76. IR (KBr, cm⁻¹): 3436(br), 3071(w), 2965(m), 2870(w), 2375(br), 1707(m), 1646(w), 1441(m), 1333(w), 1256(w), 1183(m), 1085(vs), 987(s), 770(s). DRUV-vis (nm): 219, 267. Fluorescence (λ_{ex} = 374 nm): 432 nm. ¹H NMR (400 MHz, D₂O): δ 7.19–7.21 (m, 6H, Ar-H), 3.50 (septet, 4H, *i*-PrCH, ³*J*_{HH} = 6.8 Hz), 1.16 (d, 24H, *i*-PrCH₃, ³*J*_{HH} = 6.8 Hz). ³¹P NMR (D₂O, 162 MHz): δ -4.0 ppm. TGA temp range in °C (% weight loss): 40–100 (7.0); 100–150 (4.0); 150–270 (26.4); 270–480 (22.4).

2. Mp: >275 °C. Yield: 0.36 g (69%). Anal. Calcd for [(Ba(H₂O)₇){C₁₂H₁₇PO₄}]₂ (Ba₂C₂₄H₆₂O₂₂P₂; *M*_r = 1039.34): C, 27.74; H, 6.01. Found: C, 27.90; H, 5.42. IR (KBr, cm⁻¹): 3426(br), 3069(w), 2966(m), 2869(w), 2318(br), 1644(m), 1555(m), 1438(m), 1337(w), 1257(w), 1190(m), 1085(vs), 988(m), 908(m), 770(s). DRUV-vis (nm): 219, 269. Fluorescence (λ_{ex} = 371 nm): 436 nm. ¹H NMR (400 MHz, D₂O): δ 7.17–7.20 (m, 6H, Ar-H), 3.50 (septet, 4H, *i*-PrCH, ³*J*_{HH} = 6.8 Hz), 1.16 (d, 24H, *i*-PrCH₃, ³*J*_{HH} = 6.8 Hz). ³¹P NMR (D₂O, 162 MHz): δ -3.9 ppm. TGA temp range in °C (% weight loss): 30–150 (20.7); 150–250 (12.4); 250–480 (23.6).

Synthesis of [Mg(dipp)(phen)(CH₃OH)₂]₂·(CH₃OH) (3). To a solution of Mg(OAc)₂·4H₂O (214.5 mg, 1 mmol) in methanol

(30 mL) were added solid phenanthroline (198 mg, 1 mmol) and subsequently dippH₂ (258 mg, 1 mmol). The reaction mixture was refluxed for 10 min and filtered over filter paper. Colorless square-shaped crystals were obtained from the filtrate after 3 days at 25 °C. Mp: >275 °C. Yield: 400 mg (0.74 mmol, 74%). Anal. Calcd for C₅₃H₇₀Mg₂N₄O₁₃P₂ (*M*_r = 1081.72): C, 58.85; H, 6.52; N, 5.18. Found: C, 58.21; H, 5.76; N, 5.69. IR (KBr, cm⁻¹): 3418(br), 3060(w), 2962(m), 2866(w), 1624(m), 1516(m), 1424(s), 1256(w), 1192(s), 1141(s), 1102(vs), 989(vs), 899(s), 847(m), 767(m). DRUV-vis: 266, 328 nm. Fluorescence (λ_{ex} = 379 nm, solid state): 426 nm. TGA temp range in °C (% weight loss): 70–150 (16); 150–600 (61).

Preparation of [Ca(dippH)₂(phen)₂(H₂O)₂] (4), [Sr(dippH)₂(phen)₂(H₂O)₂] (5), and [Ba(dippH)₂(phen)₂(H₂O)₂]·CH₃OH (6). These compounds were prepared by employing very similar procedures, and thus only one representative example is described. Solid Ca(OAc)₂ (158.2 mg, 1 mmol) was dissolved in a mixture of methanol/H₂O (20/10 mL), and solid phen (198 mg, 1 mmol) and subsequently dippH₂ (258 mg, 1 mmol) were added. The reaction mixture was refluxed for 3 h and filtered over filter paper. Colorless needle-shaped crystals were obtained from the filtrate after 3 days at 25 °C.

4. Mp: 185–186 °C. Yield: 350 mg (0.75 mmol, 75%). Anal. Calcd for C₉₆H₁₀₈N₈O₁₈P₄Ca₂ (*M*_r = 1866.01): C, 61.79; H, 5.83; N, 6.01. Found: C, 61.38; H, 5.85; N, 5.69. IR (KBr, cm⁻¹): 3446(br), 3060(w), 2968(s), 2866(w), 2324(br), 1624(w), 1591(w), 1513(m), 1440(m), 1424(s), 1256(m), 1182(s), 1086(m), 923(vs), 847(m), 762(s). DRUV-vis: 226, 266, 345 nm. Fluorescence (λ_{ex} = 383 nm, solid state): 420 nm. TGA temp range in °C (% weight loss): 96–170 (3); 170–585 (72). **5.** Mp: 206–210 °C. Yield: 200 mg (0.82 mmol, 82%). Anal. Calcd for C₉₆H₁₀₈N₈O₁₈P₄Sr₂ (*M*_r = 1961.09): C, 58.80; H, 5.55; N, 5.71. Found: C, 59.13; H, 5.41; N, 5.75. IR (KBr, cm⁻¹): 3433 (br), 3070(w), 2967(m), 2867(w), 2406(br), 1590(w), 1512(m), 1439(m), 1425(m), 1257(w), 1184(vs), 1079(vs), 1046(w), 921(vs), 847(m), 761(m). DRUV-vis: 226, 266, 345 nm. Fluorescence (λ_{ex} = 383 nm, solid state): 420 nm. TGA temp range in °C (% weight loss): 110–185 (1.8, -2 H₂O); 185–465 (71.2, 4 Ar moiety, 4 phen, -2 H₂O). DSC (°C): 210 (endo). **6.** Mp: 208–210 °C. Yield: 300 mg (0.52 mmol, 52%). Anal. Calcd for C₁₀₂H₁₃₆N₈O₂₆P₄Ba₂ (*M*_r = 2288.8): C, 53.53; H, 5.99; N, 4.90. Found: C, 52.68; H, 5.19; N, 4.99. IR (KBr, cm⁻¹):

(33) Kosolapoff, G. M.; Arpke, C. K.; Lamb, R. W.; Reich, H. *J. Chem. Soc., Sect. C* **1968**, 7, 815.

Investigation of Group 2 Metal–Organophosphate Interaction

3402(br), 3063(w), 2965(vs), 2867(m), 2350(br), 1622(m), 1512(m), 1425(s), 1256(s), 1184(vs), 1080(vs), 928(vs), 843(m), 767(s). UV–vis (in solid state): 226, 266, 345 nm. Fluorescence ($\lambda_{\text{ex}} = 383$ nm, solid state): 420 nm. TGA temp range in °C (% weight loss): 50–135 (3.0); 135–600 (62.0).

Single-Crystal XRD Studies. Intensity data for all of the six compounds were collected on a Oxford XCalibur CCD diffractometer at 120 K (**3**), 133 K (**5** and **6**), and 150 K (**1**, **2**, and **4**). All calculations were carried out using the programs in the *WinGX* module.³⁴ The structure solution was achieved by direct methods in each case using *SIR-92* as implemented in *WinGX*.³⁵ The final refinement of the structure was carried out using full-matrix least-squares methods on F^2 using *SHELXL-97*.³⁶ All hydrogen atom positions were found in the difference maps, and the hydrogen positions were refined with individual isotropic displacement parameters. Selected crystal data are given Table 2, and the detailed

crystallographic data for all of the structures are provided in the Supporting Information.

Acknowledgment. This work was supported by DST, New Delhi, India. S.R. thanks the DFG, Bonn, Germany, for a postdoctoral fellowship. We thank the SAIF, IIT–Bombay, and the National Single Crystal X-ray Diffraction Facility at IIT–Bombay for characterization data.

Supporting Information Available: Characterization data of IR, ³¹P and ¹H NMR (only for **1** and **2**), DRUV, and fluorescence spectra, thermal decomposition profiles for **1–6**, and details of X-ray structure investigations in CIF format. This material is available free of charge via the Internet at <http://pubs.acs.org>.

IC8003239

(34) Farrugia, L. J. *J. Appl. Crystallogr.* **1999**, *32*, 837.

(35) Altomare, A.; Casciaro, G.; Giacovazzo, C.; Gualardi, A. J. *Appl. Crystallogr.* **1993**, *26*, 343.

(36) Sheldrick, G. M. *SHELXL-97, Program for Structure Refinement*; University of Göttingen: Göttingen, Germany, 1997.